

Optimal Short Distance Electrode Locations for Impedance Pneumography Measurement from the Frontal Thoracic Area

V. Jeyhani¹, T. Vuorinen², K. Noponen³, M. Mäntysalo² and A. Vehkaoja¹

¹ Department of Automation Science and Engineering, Tampere University of Technology, Tampere, Finland

² Department of Electronics and Communications Engineering, Tampere University of Technology, Tampere, Finland

³ Faculty of Information Technology and Electrical Engineering, University of Oulu, Oulu, Finland

Abstract— Electrical impedance pneumography signal is a valuable tool in qualifying better the person's health condition. It can be used in monitoring of respiration rate, rhythm and tidal volume. Impedance pneumography has also the potential in ambulatory physiological monitoring systems that are increasingly often implemented using plaster-like on-body devices. In such cases, the area of electrode substrate may be limited and therefore, the electrode configuration, which is able to provide both a clinically valuable electrocardiogram signal and accurate pulmonary information, is an issue. EAS is a useful small area electrode configuration that can be used for electrocardiogram measurements. In this work, different two-electrode bipolar pairs of EAS system are tested for impedance pneumography measurements. Two additional electrodes are also considered in these tests. Our results show that the electrode pair S-A provides the most accurate respiration cycle length and is least affected by movement artifact. Additionally, the results show that this electrode pair produces the signals with highest amplitude.

Keywords— Pneumography, electrode, location, impedance, respiration

I. INTRODUCTION

Pulmonary measurement is a very useful tool in characterizing the person's health condition in both clinical and well-being applications. Spirometry is the gold standard monitoring technique used e.g. in clinical diagnosis to make pulmonary function tests. Even though it provides the most accurate information, it cannot be used in ambulatory conditions and it also has the drawback of partially blocking the airway. Electrical impedance pneumography (EIP), on the other hand, provides a tool for measuring impedance changes in thorax and indirectly gather pulmonary information including respiration cycle length (RCL), rhythm and tidal value [1]. There are also other techniques that can be used for acquiring some or all the aforementioned parameters. These include respiratory inductance pneumography [2], temperature sensing [3], capnography [4], using ECG [5] and photoplethys-

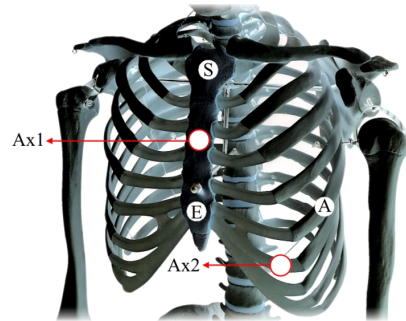


Fig. 1: Electrode locations used for measuring EIP. The locations of S, E and A are based on the EAS lead configuration. Two additional electrode locations Ax1 and Ax2 are also included in this study.

mography [6] signals for deriving respiration information.

For on-body physiological monitoring that incorporate ECG measurement, the impedance pneumography has the advantage that it can be measured using the same electrodes and thus avoiding the need to include another sensor worn by the user. Recent interest has been toward flexible and even stretchable physiological monitoring devices manufactured with printing technologies. From usability point of view, these devices need to be small sized, in which case the placement of the electrodes is a challenge, especially when clinically valuable signals, measured from a limited area of substrate, is of interest.

One possible small-area electrode configuration called EAS lead configurations is shown in Fig. 1. The electrodes E, A and S are located at the lower part of the sternum, the standard ECG V5 location, and at manubrium, respectively. In this configuration, A-S lead can approximate the clinically important CM5 lead. Also, by putting a reference electrode REF in between of A and E electrodes, A-REF and S-REF leads provide some information in addition to the A-S and E-S leads [7]. Another option is to locate the REF electrode between E and S (labeled as Ax1 in Fig. 1) which provides the lead REF-E that corresponds to the V₂S lead defined by Hurst et al in [7].

Related to this topic, various studies have been done in

which different electrode locations for measuring EIP are compared. Lahtinen et al. compared 11 different locations (using 8 electrodes) in two phases: sitting and running [8]. Their results showed that the best quality signal can be obtained by locating the electrodes on the left and right flanks. Luo et al. tested 171 electrode pairs (using 32 electrodes) and concluded that using two electrodes, one placed on sternum and another in the opposite position on the back results in the highest signal-to-motion artifact (SAR) among considered configurations [9]. Khambete et al. studied the electrode placement optimization possibilities [10]. Seppä et al. found an electrode configuration with a high impedance change-to-lung volume change linearity [11].

Most of the studies in literature report the best electrode configuration considering no limitation in the electrode locations. However, in wearable devices this issue is one of the most important restrictions. In this study, EAS electrode configuration has been studied for EIP measurements. Two additional electrodes, which have the potential to be used as a reference electrode in ECG measurement, have been included in the tests. Fig. 1 shows the tested electrode locations. All the possible combinations were tested and analyzed to find the optimal configuration from artifact and respiration estimation accuracy perspectives. We also compared the amplitude of the signal acquired from these locations with the optimal location reported in [8].

The outline of this paper is organized as follows. In section II, the measurement procedure, signal processing techniques and evaluation methods are described. The results are shown in section III. Finally, some concluding remarks are given in section IV.

II. METHODS

There were eight male subjects included in this study with the average age of 29.3 years (26 – 36 years), average height of 176.5 cm (165 – 180 cm) and average weight of 77.1 kg (60 – 93 kg). Two of the subjects were smokers. None of the participants had pulmonary problems. Body hair was removed from the electrode locations for all the subjects. Other skin preparations were not done. All the subjects were informed about the test procedure before and consents were obtained in written.

All the subjects were measured in two conditions: while sitting and during walking. The measurements for walking were done using a treadmill with a constant speed of 3 km/h and inclination of 0 degrees. Subjects were asked to keep their hands and head steady during the sitting phase, walk normally (with natural movements of hands) in the walking phase and to breathe naturally during the tests. Details about

the recording equipment and data analysis are described in the following sections.

A. Measurements

The tests were done with two separate devices simultaneously. One device was used to measure the EIP and the other to record the air temperature variations resulted by respiration. The signals measured with these devices were saved for further analysis. Each electrode pair was measured separately for around one and a half minutes to ensure one minute of unaffected signal. The electrodes connected to the EIP device were switched on the fly and signal separation was done afterwards. One annotation signal was recorded along with the main signals to ensure about the electrode switching moments. The same procedure was performed in sitting and walking phases.

The electrical impedance pneumography was measured with a custom device and using two electrodes. The hardware of the device included an analog-front-end (AFE) ADS1292R from Texas Instruments, a microcontroller, a USB connection and signal conditioning circuitry. For respiration measurement, a 32 kHz modulation signal with a phase of 112.5° was employed. The sampling rate of the device was set to 125 samples per second which activates a digital internal filter with a -3-dB frequency of 32.75 Hz in the AFE. The gain was set to 4. A graphical user interface (GUI) software developed in LabVIEW was used for receiving, real-time monitoring and saving the measured data.

The second device was used to measure the reference respiration signal with an NTC thermistor placed inside a mask that was worn in front of the mouth and nostrils during the tests. The resistance of the thermistor was measured and sent to the computer via a proprietary wireless communication protocol based on IEEE 802.15.4 standard. The signals were monitored and saved in the computer.

B. Preprocessing

After saving the signals in the computer, they were processed to be ready for evaluation. Since the temperature signal has the sampling rate of 250, the impedance signal was interpolated linearly by a factor of 2.

Both of the signals, impedance and temperature were filtered by a high-pass IIR filter and a low-pass FIR filter. The low-pass filter was designed to have the stop-band and pass-band frequencies of 0.01 and 0.02 Hz, respectively. The low-pass filter was set to perform with pass-band and stop-band frequencies of 2 and 3 Hz, respectively. The filtering process was done by forward-backward filtering technique to prevent the effect of non-linear phase response of the IIR filter.

C. Evaluation

Two different factors were considered to determine the best electrode configuration for EIP. The RCLs were calculated from the impedance signals and compared to the one derived from the temperature sensor. Additionally, measurement sensitivity was evaluated by comparing the amplitudes of the impedance pneumography signals recorded from different electrode locations.

Calculation of respiration cycle length (RCL): First, all the signals were divided into 12-second frames with 6 seconds overlap. Therefore, for each 1 minute measurement, 9 frames, each consisting of 3000 samples, were constructed. The frame size was found such that the signal can be considered stationary while it includes enough number of periods of signal. The frames were then analyzed using the short-time autocorrelation function (ACF), which is defined as

$$r(\tau) = \sum_{n=0}^{N-1-\tau} x(n)x(n+\tau), \quad (1)$$

where $x(n)$ is one frame of the signal and τ is the lag. The result of ACF was then processed by a local peak detection function which was restricted to find the peaks with two following criteria:

- the peak should be more than 2 seconds apart and less than 12 seconds. The 12 second limit is set by the length of the frame.
- the peak should have positive amplitude

The location of the peak closest to the mid-point of the ACF was considered as the period of the signal. The results of RCL calculation from both devices were compared by the mean absolute error (MAE) and mean error (bias, also known as systematic error) measures. MAE is defined as

$$MAE = \frac{1}{N} \sum_{n=1}^N |\hat{y}[n] - y[n]| \quad (2)$$

and mean error as

$$ME = \frac{1}{N} \sum_{n=1}^N (\hat{y}[n] - y[n]), \quad (3)$$

where \hat{y} and y indicate the impedance signal and the reference signal measured with the temperature sensor in both equations, respectively.

The algorithm was designed to return a NaN (not a number) value, when no point could be found with the given criteria. These values were then ignored in calculation of errors.

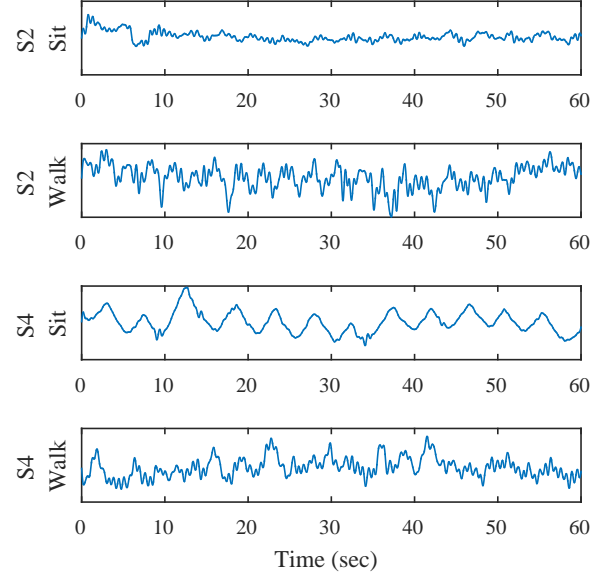


Fig. 2: Impedance signals recorded from electrode location S-Ax2 and subjects 2 and 4 in walking and sitting phases.

The number of occurrence of NaN values is reported in the results for each electrode location.

Amplitude of the recorded signal: This factor was used to find out which electrode location is more affected by the respiration and thus produces the higher amplitude variation. The respiration amplitude was calculated by finding the value of magnitude spectrum of the signal at the frequency of respiration. This task was performed as a frame-wise process. The final results (for each subject and electrode location) were then calculated as the mean value of all the frames. The spectrum was calculated using fast Fourier transform (FFT) with 2^{20} spectral bins. The respiration frequency was defined as the frequency of the peak in the magnitude spectrum which is closest to the respiration frequency defined from the autocorrelation signal. The magnitude of this point was considered as the magnitude of the respiration component.

For comparison purposes, one EIP measurement was performed by placing two electrodes on the right and left sides of the body, on the midaxillary lines, about 10 centimeters lower than underarms. This signal was recorded only for subject number 1 and was used to compare the amplitude of the EIP signals recorded from the EAS electrode configuration and this optimal (as stated in [8]) electrode pair.

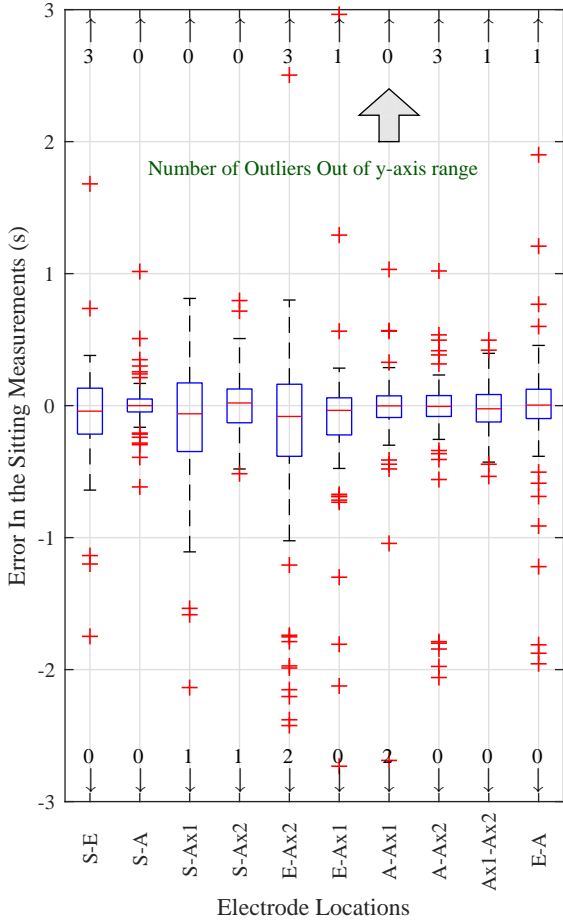


Fig. 3: Difference between the respiration cycle lengths obtained from the EIP and reference signals for all the subjects in every electrode pair combination in sitting position. The box edges represent the 25th and 75th percentile of the data set. The center value represents the median value and the floating hollow circles indicate the outliers. The numbers close to the small vertical arrows indicate number of outliers which are located out of the y-axis range.

III. RESULTS AND DISCUSSION

All the subjects were measured in the same environment and with the same procedure. After saving the signals, they were moved to MATLAB (2015b) from MathWorks Inc. The results of evaluations are presented in the following.

Fig. 2 shows examples of impedance signals recorded from subjects 2 and 4. Movement artifacts in walking phase can be clearly seen as higher frequencies in the signals, especially in the signal recorded from subject 2. The y-axis unit of the impedance signal is arbitrary but the scale is the same in all four panels.

Fig. 3 and Fig. 4 show the error of RCL detection from all the electrode locations in sitting and walking measure-

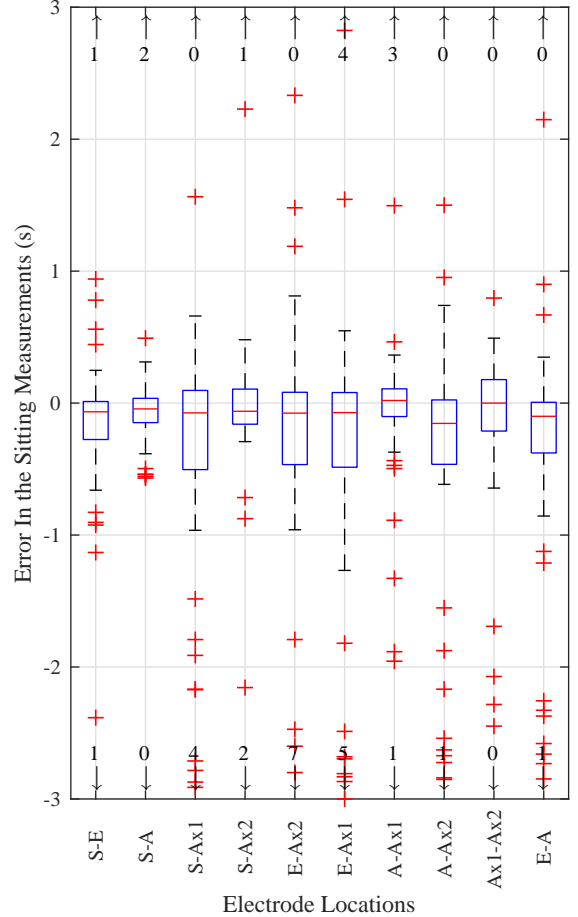


Fig. 4: Difference between the respiration cycle lengths obtained from the EIP and reference signals for all the subjects in every electrode pair combination during walking. The plot specifications are similar to ones mentioned for 3

ments, respectively. The errors are calculated as $\hat{\phi} - \phi$, where ϕ and $\hat{\phi}$ are the RCLs in one frame of the signal calculated from temperature and EIP measurements, respectively. For one of the subjects the recording for the E-A location was only 32 seconds (instead of 60 seconds). Thus 4 frames were constructed for this measurement (instead of 9) and were padded by NaN (not a number) values to be able to concatenate it with the rest of the results. Therefore, there were totally $72 - 5 = 67$ frames of signal for each electrode location. In these figures, each box represents error of measurements from each electrode location, the central mark shows the median value and the box edges indicate the 25th and 75th percentiles. The whiskers extend to the most extreme point not considered as outlier. The data points are drawn as outliers if they are larger than $p_2 + 1.5(p_2 - p_1)$ or smaller

Table 1: Mean absolute error (MAE) and mean error (ME) of RCL calculated from EIP with respect the results from the temperature-based measurement device. NaN columns show the number of missing respiration periods from EIP measurements out of total number of frames for each electrode location, which is 67. This corresponds to the number of NaNs produced by the algorithm used for RCL calculation

Electrode Location	Sit MAE	Walk MAE	Sit ME	Walk ME	Sit NaN	Walk NaN
S-E	0.513	0.452	0.183	-0.095	2	0
S-A	0.113	0.260	0.008	0.045	0	0
S-Ax1	0.396	0.697	-0.198	-0.516	2	0
S-Ax2	0.263	0.408	-0.070	-0.063	0	0
E-Ax2	0.871	0.799	-0.217	-0.505	0	0
E-Ax1	0.404	1.075	-0.075	-0.207	3	0
A-Ax1	0.272	0.590	-0.127	0.127	0	0
A-Ax2	0.460	0.566	0.094	-0.420	0	0
Ax1-Ax2	0.192	0.305	0.035	-0.096	0	0
E-A	0.334	0.539	-0.010	-0.392	0	0

than $p_1 - 1.5(p_2 - p_1)$, where p_1 and p_2 are the 25th and 75th percentiles, respectively. The results from Fig. 3 clearly show that S-A electrode locations provide the smallest error i.e. the most accurate RCL in sitting condition. It can be seen that the locations S-Ax1 and E-Ax2 produce almost the worst accuracy for RLC detection. The outliers in S-E, E-Ax2 and A-Ax2 configurations illustrate that these locations are more prone to produce sporadic large error, at least with the algorithm used. The same conclusions can be found from Fig. 4. Again S-A shows the best results. The S-Ax1, E-Ax2, E-Ax1 and A-Ax2 represent the worst cases. Also, it is worth mentioning that in the walking phase, the auto-correlation method for measuring the RCL tends to produce more number of negative errors than positive (underestimates the RCL).

Mean absolute error (MAE) and mean of the errors of the RCL calculated from EIP are presented in Table. 1. The table shows that the smallest error for all the cases is generated from S-A electrode location. NaN columns show the number of times that the mentioned algorithm failed to assigned a period (with given criteria) to a frame of the signal (out of 67). The S-E electrode configuration shows two failures of period detection which has happened in measurements from two different subjects (subjects 2 and 4). The same issue was observed for S-Ax1 electrode pair for the same subjects. All the three failures for E-Ax1 have occurred for subject 4. These observations could be expected because the electrodes S, Ax1 and E are placed on sternum and the impedance between them is probably less affected by the changes of the volume of the lungs. Although, these failures might also be

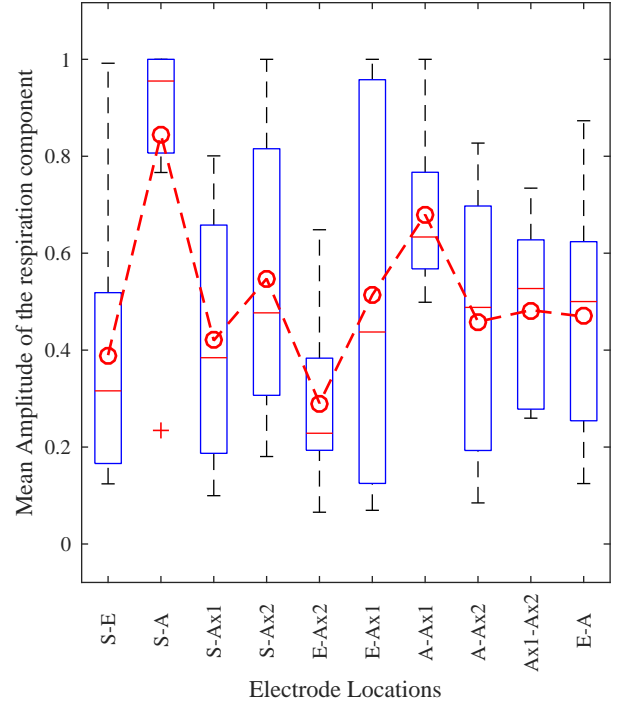


Fig. 5: Amplitude of the respiration component from different subjects and in different electrode locations. The y-axis represents an arbitrary unit of EIP. The values in each group of values are resulted from mean of respiration amplitude in different frames of the corresponding signal. The dashed red line shows the mean values in each group of data.

due to large artifacts/noise in the signals.

Fig. 5 illustrates the result of magnitude analysis of the impedance signals recorded from different locations and subjects in sitting phase. Relatively large subjectwise variations were noticed in the amplitude of the signals and therefore the comparison was done for signals normalized for each subject. The normalization is done by dividing all the magnitude values by their maximum number for each subject. The specifications of this box plot are the same as in Fig. 3 and Fig. 4. The red dashed line represents the mean values in each group of data. It can be seen that the electrode pair S-A has produced the strongest signals with the highest mean and median of the respiration magnitude values. Additionally, it is noticeable that the signals recorded from this electrode pair had least intra- and inter-subject variability in amplitude and were least affected by the small mismatches in the electrode locations between different subjects. It is worth emphasizing that only the signals recorded in the sitting position were used in this analysis.

Fig. 6 shows the EIP signal recorded from the optimal electrode locations found in [8] (right and left flanks) and

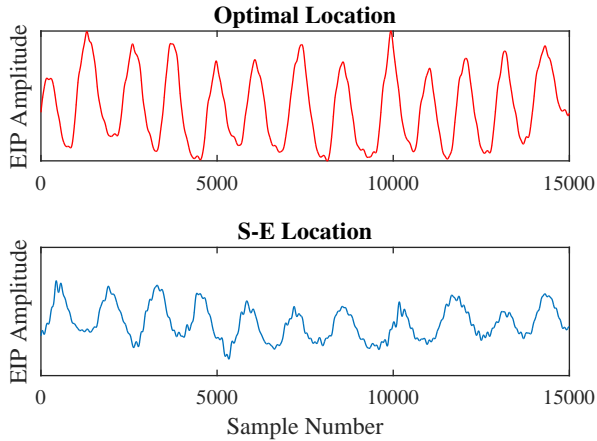


Fig. 6: The EIP signals recorded from the optimal and S-A electrode locations. The signals were recorded in the sitting position. The y-axes have an arbitrary unit, but the scale is the same in both images.

compares it with the S-A electrode location. The signals were recorded from the first subject in the sitting phase. The y-axes have an arbitrary unit, but the scale is the same for both panels. It can be seen that the optimal electrode location provides stronger signal. However, S-A can act as a good alternative in wearable devices.

IV. CONCLUSION

In this work ten different electrode pairs (using five electrodes) in EAS configuration for eight subjects for measuring electrical impedance pneumography were tested. The main aim of the study was to find the electrode pair which is the most influenced by the respiration and provides the largest robustness to movement artifacts.

The results show the electrode pair S-A provides the most accurate respiration cycle length (RCL) calculation among the ten configurations considered, in which electrodes S and A are located at manubrium and the standard ECG V5 location, respectively. Additionally, it is presented that this electrode pair produces the strongest signal and is least affected by movement artifact and most sensitive to the respiration components. Further, this electrode pair has least intra- and inter-subject variability.

There might be some variations in the results by using different RCL calculation methods. Also, suitability of stretchable electrodes manufactured with screen printing technology for respiration monitoring should be tested.

The future work will include testing the same electrode configurations for female subjects. Also, the effect of different methods for RCL detection will be analyzed.

ACKNOWLEDGEMENTS

This research was funded by the Finnish Funding Agency for Innovation (Tekes) and several Finnish companies as a part of VitalSens project. Funding decision number: 40103/14 and 40104/14

REFERENCES

- Freundlich J. J., Erickson J. C.. Electrical impedance pneumography for simple nonrestrictive continuous monitoring of respiratory rate, rhythm and tidal volume for surgical patients *CHEST Journal*. 1974;65:181–184.
- Hill S. L., Blackburn J. P., Williams T. R. Measurement of respiratory flow by inductance pneumography *Medical and Biological Engineering and Computing*. 1982;20:517–518.
- AL-Khalidi F. Q., Saatchi R., Burke D., Elphick H., Tan S. Respiration rate monitoring methods: A review *Pediatric pulmonology*. 2011;46:523–529.
- Schéele B. H. C. Von, Schéele I. A. M Von. The measurement of respiratory and metabolic parameters of patients and controls before and after incremental exercise on bicycle: supporting the effort syndrome hypothesis? *Applied Psychophysiology and Biofeedback*. 1999;24:167–177.
- Mirmohamadsadeghi L., Vesin J. M. Respiratory rate estimation from the ECG using an instantaneous frequency tracking algorithm *Biomedical Signal Processing and Control*. 2014;14:66–72.
- Leonard P. A., Douglas J. G., Grubb N. R., Clifton D., Addison P. S., Watson J. N. A fully automated algorithm for the determination of respiratory rate from the photoplethysmogram *Journal of Clinical Monitoring and Computing*. 2006;20:33–36.
- Willis Hurst J. Would Different Routine Precordial Electrode Positions Be More Useful? Answer: Not Likely *Clin Cardiol*. 2009;32:58–64.
- Lahtinen O., Seppä V. P., Väisänen J., Hyttinen J. Optimal electrode configurations for impedance pneumography during sports activities *4th European Conference of the International Federation for Medical and Biological Engineering*. 2009:1750–1753.
- Luo S., Afonso V. X., Webster J. G., Tompkins W. J. The electrode system in impedance-based ventilation measurement *Biomedical Engineering, IEEE Transactions*. 1992;39:1130–1141.
- Khambete N., Metherall P., Brown B., Smallwood R., Hose R. Can we optimize electrode placement for impedance pneumography? *Annals of the New York Academy of Sciences*. 1999;873:534–542.
- Seppä V. P., Hyttinen J., Uitto M., Chrapek W., Viik J. Novel electrode configuration for highly linear impedance pneumography *Biomedizinische Technik/Biomedical Engineering*. 2013;58:35–38.

Author: Vala Jeyhani
 Institute: Tampere University of Technology
 Street: Korkeakoulunkatu
 City: Tampere
 Country: Finland
 Email: vala.jeyhani@tut.fi